Supporting Information

Porous Platinum-Silver Bimetallic Alloy: Surface Composition, Strain Tunability and Enhanced Electrocatalysis

Erhuan Zhang,[a] Fenfen Ma,[b] Jia Liu,[a,*] Jingyao Sun,[c] Wenxing Chen,[a] Hongpan Rong,[a] Xiyue Zhu,[a] Jiajia Liu,[a] Meng Xu,[a] Zhongbin Zhuang,[c] Shilv Chen,[b] Zhenhai Wen,[d] and Jiatao Zhang[a,*]

a. Beijing Key Laboratory of Construction Tailorable Advanced Functional Materials and Green Applications, School of Materials Science and Engineering, Beijing Institute of Technology, Beijing 100081, PR China

b. Conversion Materials, Key Laboratory of Cluster Science of Ministry of Education, Beijing Key Laboratory of Photoelectronic/Electrophotonic School of Chemistry and Chemical Engineering, Beijing Institute of Technology, 100081 Beijing, China

c. State Key Lab of Organic-Inorganic Composites, Beijing Advanced Innovation Center for Soft Matter Science and Engineering, Beijing Key Lab of Energy Environmental Catalysis, Beijing University of Chemical Technology, Beijing 100029, China

d. CAS Key Laboratory of Design and Assembly of Functional Nanostructures, and Fujian Provincial Key Laboratory of Nanomaterials, Fujian Institute of Research on the Structure of Matter, Chinese Academy of Sciences, Fuzhou, Fujian 350002, China

E-mail address: zhangjt@bit.edu.cn.

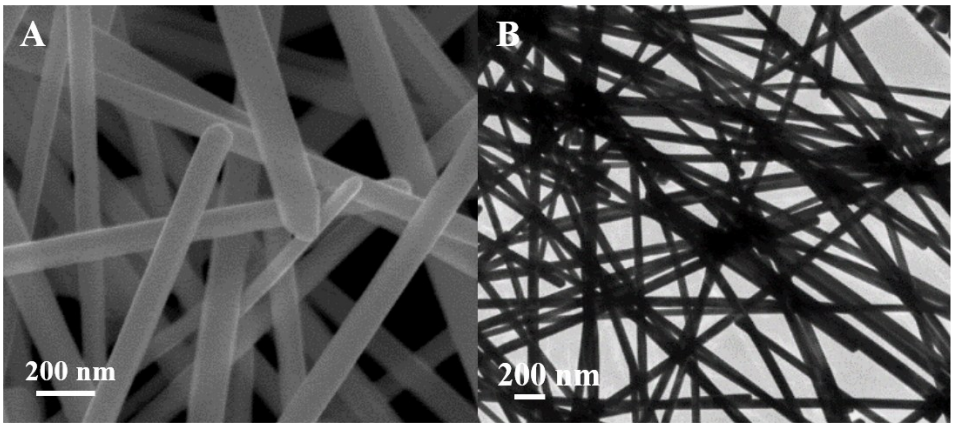

Figure S1. SEM and TEM of Ag nanowires.

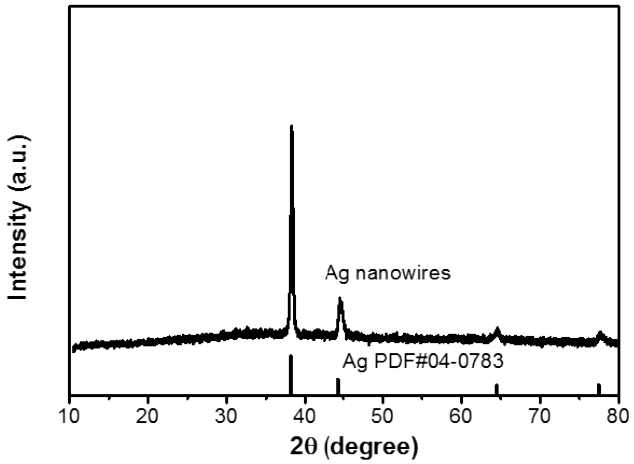

Figure S2. XRD of Ag nanowires.

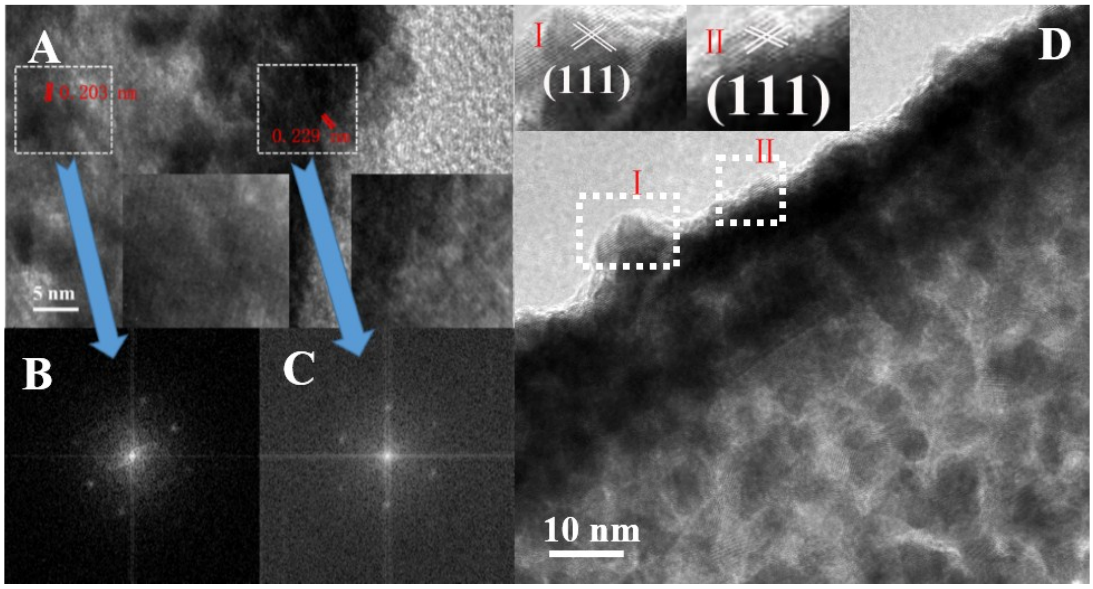

Figure S3. HRTEM images of PtAg-4 nanotube where inserts are the magnified views of areas for the determination of the lattice fringes. Bottom images (B and C) are the corresponding Fourier transform patterns of the selected area in the frame presented upwards. The edge of PtAg-4 nanotube (inset of D) is their (111) facet, which is consistent with the results from the image (left).

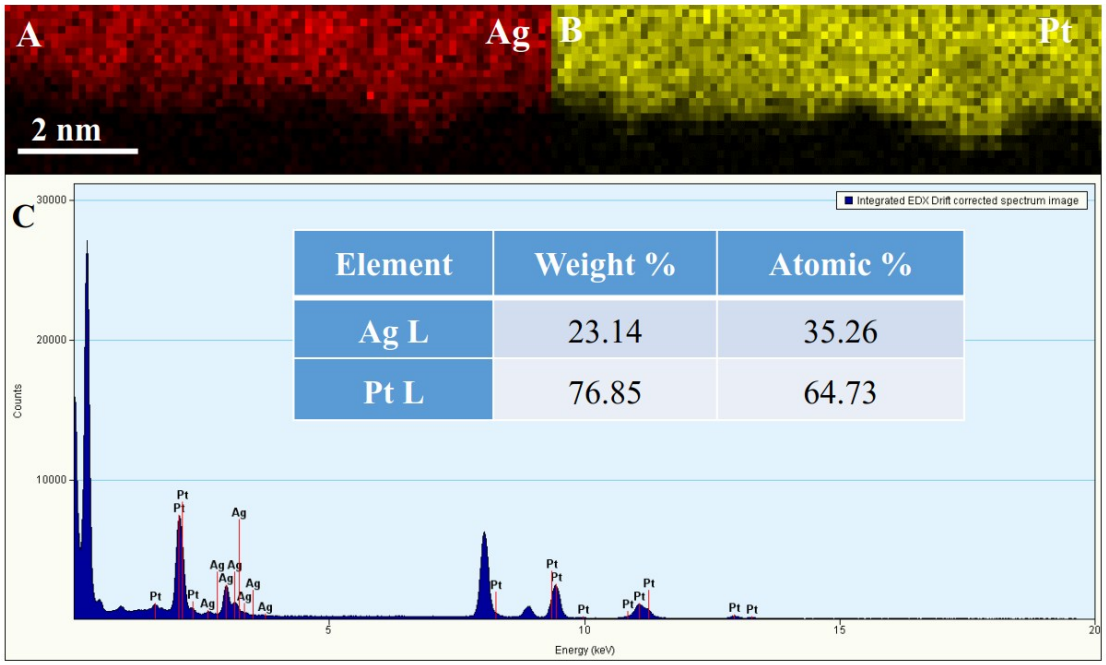

Figure S4: The HAADF-STEM elemental maps Ag (A) and Pt (B) of as-synthesized PtAg-4 bimetallic nanoalloy. (C) The corresponding STEM-EDS and element ratio.

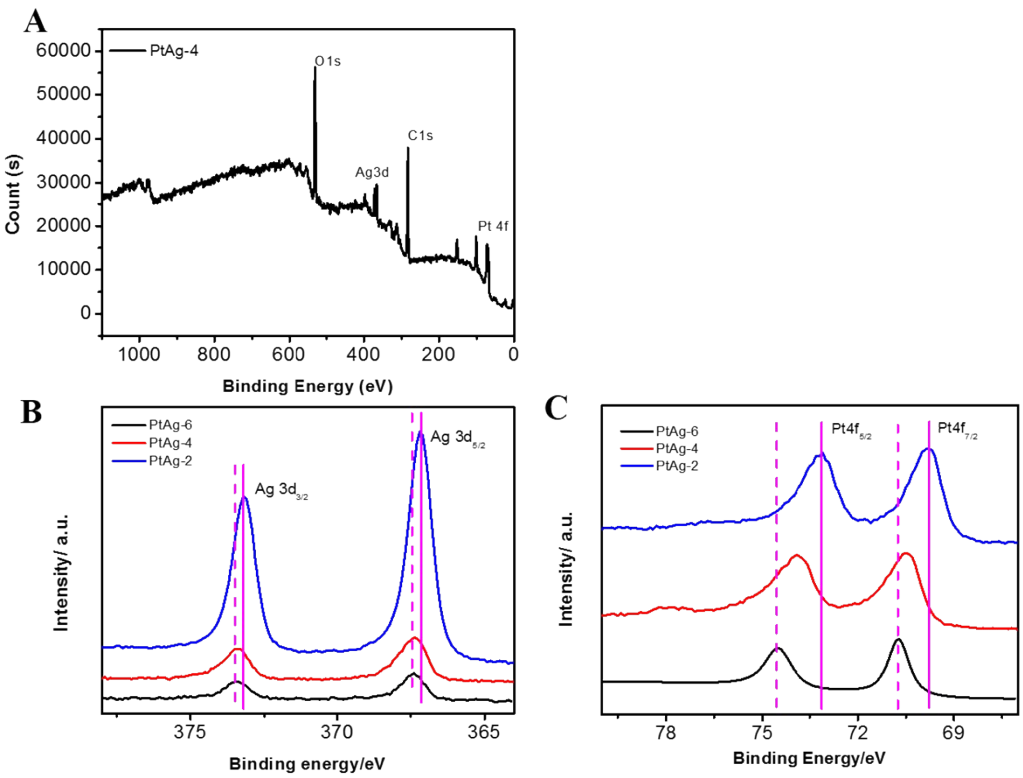

Figure S5. (A) XPS survey spectrum of the PtAg-4 nanotubes, comparison of the Ag 3d (B) and Pt 4f (C) XPS spectra of PtAg-n (n=2, 4, 6) nanotubes.

Samples	The ratio of Ag: Pt at surface from XPS
PtAg-2	10.43/3.94
PtAg-4	2.44/3.92
PtAg-6	1.94/5.91

Table S1. The surface composition of PtAg-2 NTs, PtAg-4 NTs and PtAg-6 NTs analyzed from XPS.

Samples	Pt mass (%)	Catalysts	Pt mass (%)
Pt/C	20.0	Pt/C	20.0
Pt-Ag-2	28.73	Pt-Ag-2/C	14.9
Pt-Ag-4	47.63	Pt-Ag-4/C	19.1
Pt-Ag-6	63.83	Pt-Ag-6/C	19.5

Table S2. The bulk composition of PtAg-2, PtAg-4 and PtAg-6 analyzed from ICP-MS.

Element	Weight%	Atomic%
C K	6.69	40.86
Si K	2.00	5.22
Ag L	64.51	43.85
Pt M	26.79	10.07
Totals	100.00	

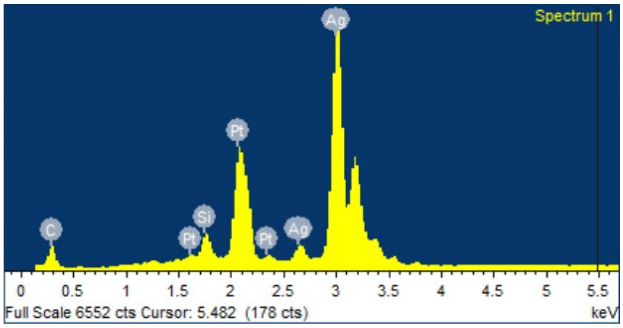

Element	Weight%	Atomic %
C K	10.98	56.66
Si K	3.37	7.42
Ag L	33.95	19.50
Pt M	51.69	16.42
Totals	100.00	

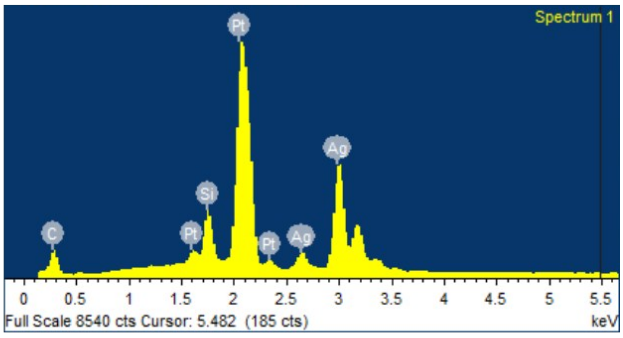

Element	Weight%	Atomic%
C K	20.74	62.96
O K	1.49	3.40
Si K	14.76	19.16
Ag L	17.85	6.03
Pt M	45.16	8.44
Totals	100.00	

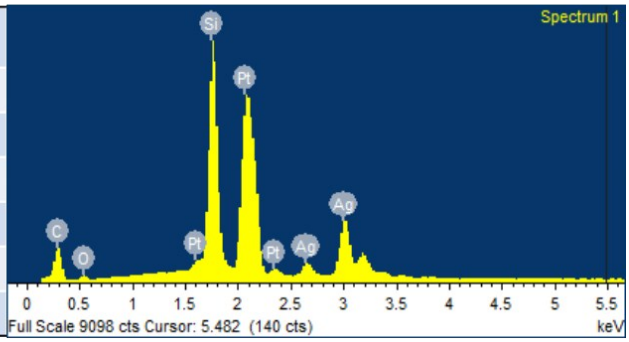

Figure S6. EDS of (A) AgPt-2 NTs, (B) AgPt-4 NTs, and (C) AgPt-6 NTs.

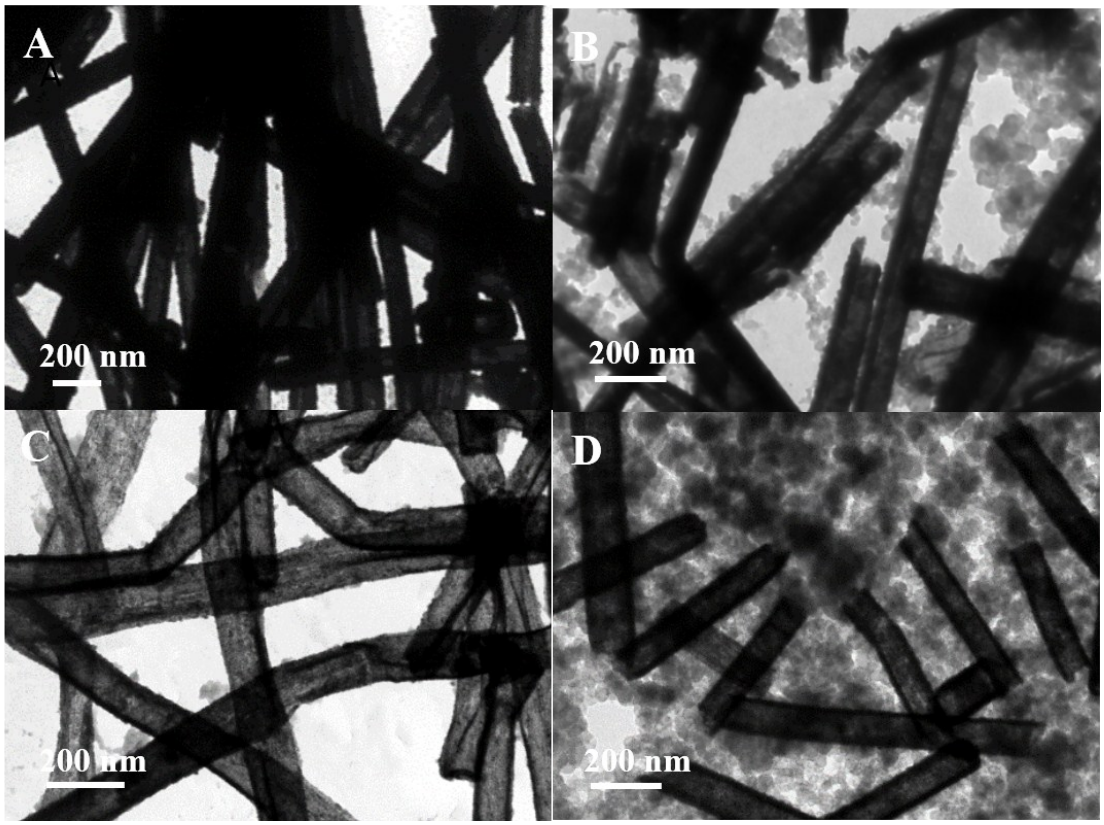

Figure S7. TEM images for PtAg-2 NTs (A, B) and PtAg-6 NTs (C, D) before and after the addition of carbon support.

A

Element	Weight %	Atomic %
Ag L	27.60	47.00
Pt L	72.4	53.00
Totals	100	

B

Element	Weight %	Atomic %
Ag L	32.90	40.81
Pt L	67.10	59.19
Totals	100	

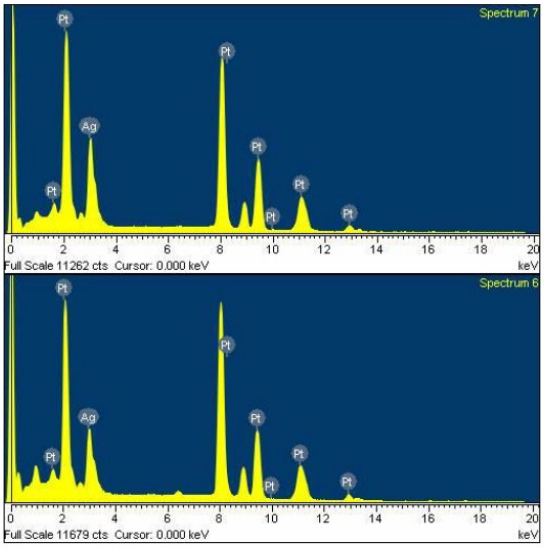

Figure S8. Average bulk compositions of PtAg-4 NTs at different activation cycles: (A) 50 cycles and (B) 150 cycles by EDS analysis.

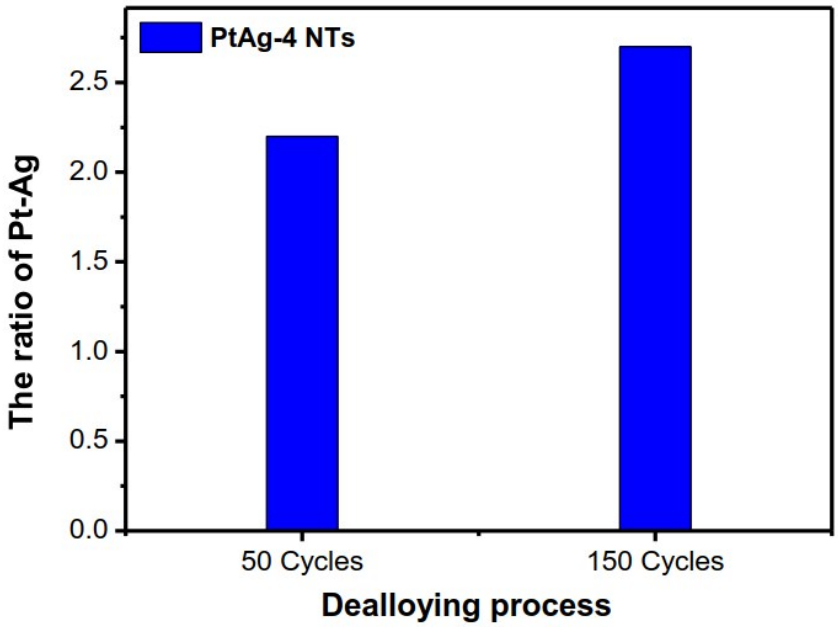

Figure S9. Surface compositions of PtAg-4 NTs at different activation cycles: 50 cycles (A) and 150 cycles (B) by XPS analysis.

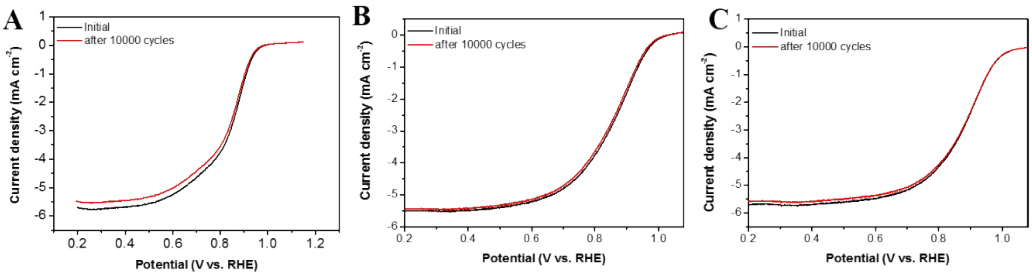

Figure S10. The accelerated durability test (ADT) for the commercial Pt/C (A), PtAg-2 NTs/C (B) and PtAg-6 NTs/C (C) in an O_2-saturated 0.1 M $HClO_4$ aqueous solution with a sweep rate of 100 mV/s.

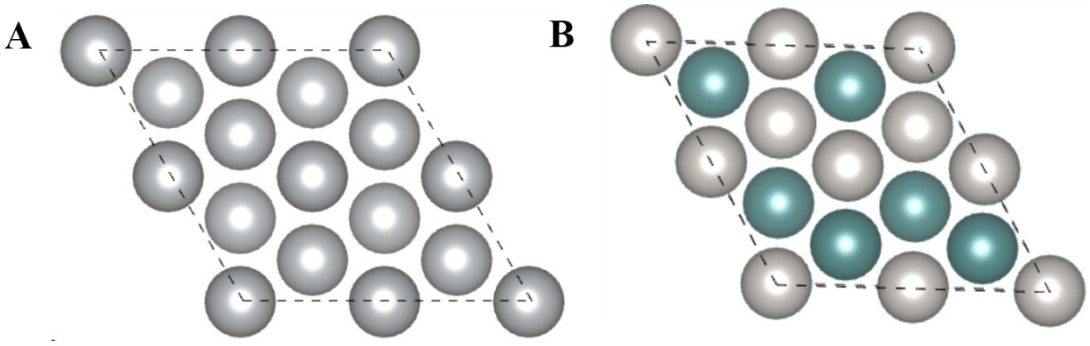

Figure S11. Top views of the surfaces on Pt (111) and PtAg-4 NTs alloy (111) models (Green and gray balls represent the Ag and Pt atoms).

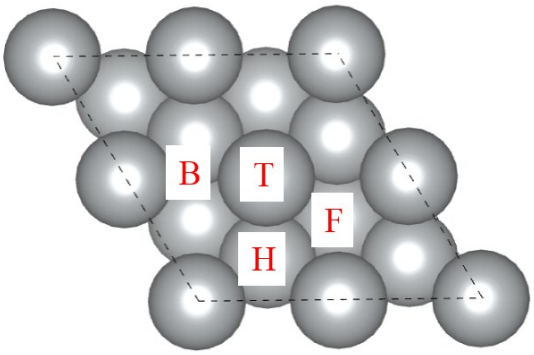

Figure S12. Hard sphere models of pure Ag (111) and Pt (111) surfaces, T: top, B: bridge, H: hcp-hollow, F: fcc-hollow, H_1 and H_2: hcp-hollow and the O atom is sit on the above of Ag and Pt atom, respectively.

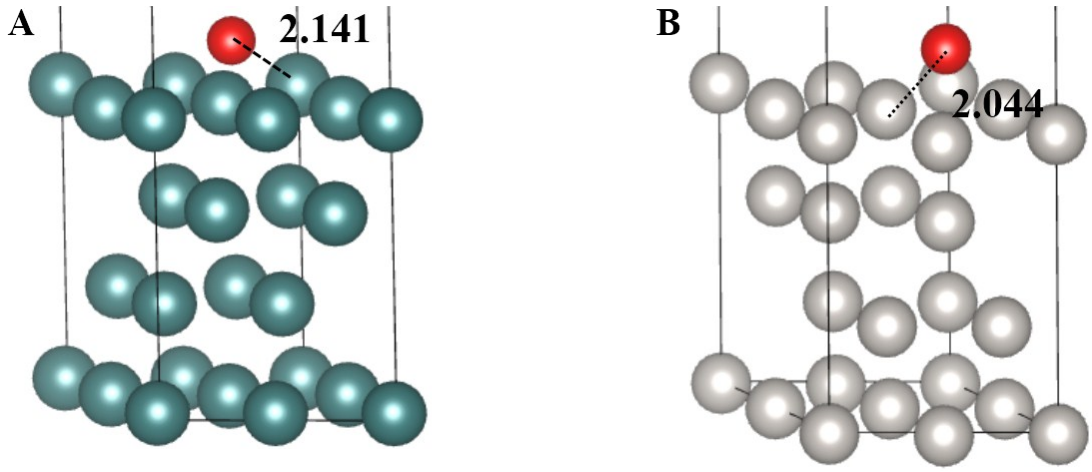

Figure S13. The favorable adsorption configurations for O adsorbed on the (A) Ag (111), (B) Pt (111) surfaces.

Table S3. Comparison of ORR performance in acidic media for PtAg-4 NTs with other noble metal electrocatalysts.

Catalyst type	ECSA ($m^2 g^{-1}$)	Mass activity ($A mg^{-1}_{Pt}$)	Specific activity($mA cm^{-2}_{Pt}$)	References
PtCo NWs		0.26	1.2	Nano Energy 2014, **10**, 135-143.
PtAg nanocages/C	50.2	0.64	1.23	Nano Lett. 2016, **16**, 6644-6649.
Pt/PtTe NWs		0.265	0.77	Chem. Mater. 2016, **28**, 8890-8898.
Au rod@Pt	141.6	0.128 (at 0.8 V)	0.09	Angew. Chem. Int. Ed. 2010, **49**, 10197-10201.
Pt NW/C		0.12	0.275	Adv. Mater. 2008, **20**, 3900-3904.
PtAg HNCNs	70.1	0.37(0.81)	0.66	Electrochemical Acta 2017, **245**, 883-892.
Pt NTs/NG	44.82	0.35	0.771	Nano Energy 2015, **13**, 318-326.
PtAgBiCo/C	42	0.81	1.95	Chem. Sci. 2017, **8**, 4292-4298.
PtP NTAs	26.7			Chem. Sci. 2015, **6**, 3211-3216.
PtPdCu ANNTs	78.1	0.523	0.67	Adv. Energy Mater. 2012, **2**, 1182-1187.
$Pt_{76}Cu_{24}$BANTs	49	0.41	0.83	RSC Adv., 2016, **6**, 69233-69238
Au/PtAu Nanotubes	22.3	0.237	1.218	Chem. Eur. J. 2015, **21**, 7556-7561
PtAg-4 NTs/C	60.4	0.688	1.13	**This work**